FRACTURE BEHAVIOR OF UNIAXIAL FLOWED SAND COLUMN WITH SURCHARGE FILTER

Philipp Schober[1] & Conrad Boley[1]

[1] Institute for Soil Mechanics and Geotechnical Engineering, Universität der Bundeswehr München, Germany,
Werner-Heisenberg-Weg 39, 85577 Neubiberg
E-mail: philipp.schober@unibw.de

Abstract

Experimental studies on hydraulic heave with surcharge filter on the excavation side of the wall have shown that the thickness of the surcharge filter has a considerable influence on the failure-mechanism. For further investigation, one-dimensional flow experiments that enable a better understanding of the influence of a surcharge filter on the failure-mechanism were conducted. In these experiments, the observations were focused primarily on the influence of the surcharge filter thickness and relative density of the sand on the critical hydraulic gradient. Furthermore the actual fracture process was closely analyzed.
This paper shows the test results of the experimental series and presents first finding.

Introduction

Due to new technical expertise for the hydraulic heave safety at excavation walls with a surcharge filter on the excavation side of the wall according to Odenwald and Herten (Odenwald and Herten, 2008), the Institute for Soil Mechanics and Geotechnical Engineering of the Bundeswehr Universität München carried out numerous laboratory tests to simulate hydraulic heaves with surcharge filters on the excavation side of the wall. During the test series, the fracture behavior of the hydraulic heave was observed by several measurement techniques. By analyzing the test results, it was found, that the thickness of the surcharge filter has a significant influence on the fracture behavior and the critical potential difference Δh. (Schober, 2011) (Schober et al, 2011).
To analyze the influence of the surcharge filter thickness on the fracture behavior for the hydraulic heave safety in more detail, the Institute for Soil Mechanics and Geotechnical Engineering of the Universität der Bundeswehr München in cooperation with the Federal Waterways Engineering and Research Institute in Karlsruhe performed uniaxial flow tests with surcharge filter.

Description of the Laboratory Experiments

Construction of the test rig

To visualize the fracture behavior and to verify the theoretical approach, we designed a specific apparatus to simulate uniaxial flow through a sand column (Figure 1). The test rig consists of two parts: the test cylinder (a) und the water supply (b), which is used to increase the potential difference continuously.
(a): The cylindrical test box has a height of 60 cm and a diameter of 19 cm. It consists mainly of an acrylic glass cylinder and a funnel shaped base plate. An inlet in the middle of the base plate connects the test box with the water supply. At a height of 50 cm, an oval hole in the cylinder serves as a discharge unit with a width of 3 cm allowing free drain.
(b): The water supply consists of a box with an installed overfall and a staff gauge to regulate the potential difference Δh. Altogether is placed on a hand lift truck to change the potential difference continuously. The water supply and the test cylinder are connected by a pipe (∅ 3 cm).

Test material

Sand (as basic material) and a mixture of coarse sand and fine gravel (as filter material) were used as test material for the uniaxial flow tests with surcharge filter on the top of the sand column.
As basic material, sand with a closeness of grain of ρ_S = 2.72 g/cm³ and a grain size distribution of 0.1 mm to 1.0 mm was used. The sand can be classified as uniform fine- to medium-graded sand. The coefficient of permeability k_f = 5.83 x 10^{-5} m/s was determined.
The surcharge filter consists of coarse sand and fine gravel with a closeness of grain of ρ_F = 2,70 g/cm³ and with a grain size distribution from 0.6 mm to 7.0 mm. For the selection of the filter material, the filter rule according to Terzaghi (1948) was chosen.

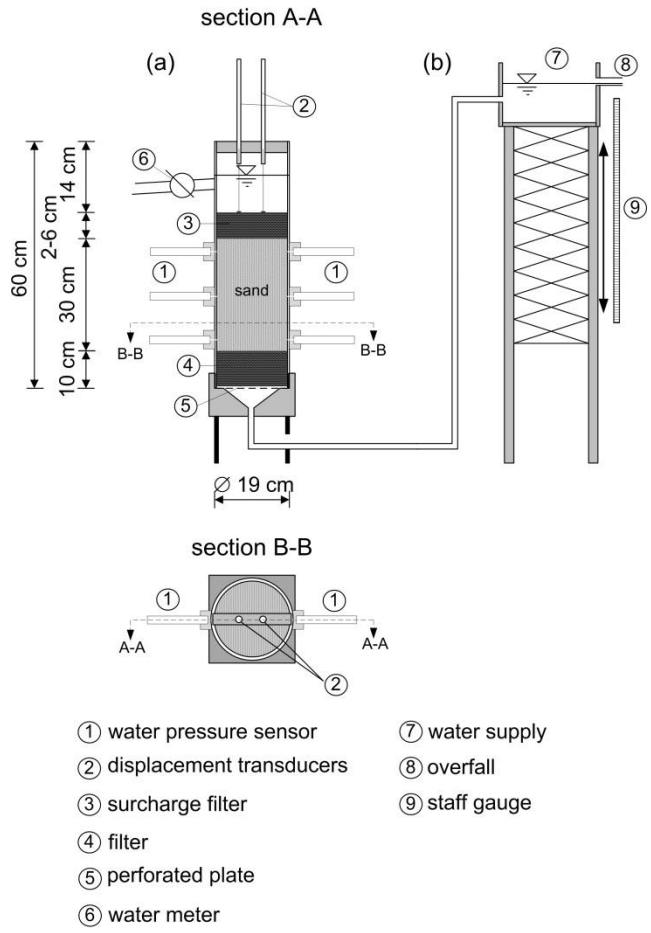

Figure 1: Construction of experimental rig

Test procedure

The sand was filled into the test cylinder in 1 cm thick layers. To reach the default relative densities of D = 0.1, 0.5 and 0.8 the dry mass per layer had to be determined. The sand was filled into the box underwater and was compacted by a stemmer. The height of one sand layer was checked with the help of marks placed on the walls of the test cylinder.

The surcharge filter was filled into the cylinder similar to the sand, with the identical relative density as the sand and also in 1 cm thick layers.

Altogether, we carried out 25 tests. The effective density was varied between D = 0.1, 0.5 und 0.8. Moreover, the surcharge filter was installed in different sizes, with a thickness of d_F = 1, 2, 3, 4, 5 and 6 cm. Also tests without a surcharge filter were carried out. In the test series, the different effective densities of the sand were combined with the different sizes d_F of the surcharge filter.

At the beginning of each test, the water level in the water supply was on the same level as in the test cylinder. Hence, there were no flow forces acting on the sand. The test was started by switching on all measuring instruments at the same time. This was necessary to permit a direct comparison of all measurement techniques. At first, the potential difference Δh was raised in 5 cm steps. If the potential difference Δh got closer to the critical value, the potential difference was raised in 1 cm and in 0.5 cm steps toward the end. The hydraulic difference Δh was increased up to the collapse of the sand column. The duration of one step was defined individually by using the measuring curves from the water pressure sensors. When the potential curves of the water pressure sensors were deflected after an increase of the potential difference Δh, it was assumed that a steady flow had occurred. At this point the next potential step was introduced.

Theoretical fracture behavior

According to Terzaghi (1948) a vertical streamed sand column collapses if the flow forces exceed the buoyant unit weight of the sand column. This is valid if all friction forces are negligible. The critical state can be described by the critical hydraulic gradient i_{crit}.

Theoretical critical hydraulic gradient

The equilibrium in the sand column and in critical condition is:

$$l \cdot \gamma'_S = \Delta h_{crit} \cdot \gamma_W \qquad (1)$$

where γ'_S is the buoyant unit weight of the sand, l is the length of the sand column, Δh_{crit} is the hydraulic difference in critical condition and γ_w is the unit weight of the water.

If $\gamma'_S = \gamma_w$, the critical hydraulic difference in critical condition is $\Delta h_{crit} = l$.

The critical hydraulic gradient i_{crit} is defined by:

$$i_{crit} = \frac{\Delta h_{crit}}{l} \qquad (2)$$

If a surcharge filter is installed and the head lost in the filter is negligible, the equilibrium equation (1) in critical condition can be extended as following:

$$d_F \cdot \gamma'_F + l \cdot \gamma'_S = \Delta h_{crit} \cdot \gamma_W \qquad (3)$$

where γ'_F is the buoyant unit weight of the surcharge filter and d_F is the thickness of the surcharge filter. If $\gamma'_S = \gamma_w = \gamma'_F$, the critical hydraulic difference is $\Delta h_{crit} = l + d_F$. The critical hydraulic gradient i_{crit} with surcharge filter is defined by:

$$i_{crit} = \frac{\Delta h_{crit}}{l} = \frac{d_F + l}{l} \qquad (4)$$

Vertical effective stresses

Sequentially the theoretical stress level in the sand column and, if present, in the surcharge filter is analyzed. Therefore the stresses in the sand column are displayed in Figure 2 and 3 prior to the beginning of the fluid flow (i = 0), for hydraulic gradients $i < i_{crit}$ and at least for the critical hydraulic gradient $i = i_{crit}$. This also was already studied by Tanaka and Toyokuni (1991).

Vertical effective stresses without surcharge filter

The vertical stresses in the sand column for different hydraulic gradients i are shown in Figure 2.

Before the fluid flow starts (i = 0), the vertical effective stresses in the base of the sand column are $\sigma'_{v,b} = \gamma'_S \cdot l$. The effective vertical stress on the sand surface are $\sigma'_{v,s} = 0$.

If the potential difference is raised up to $\Delta h < \Delta h_{crit}$, the vertical effective stresses on the base of the sand column are reduced to $\sigma'_{v,b} = \gamma'_S \cdot l - \Delta h \cdot \gamma_w$. The effective vertical stresses $\sigma_{v,s}$on the sand surface are still zero.

When the potential difference reaches the critical value Δh_{crit}, that is, if the hydraulic gradient i is equal to the critical hydraulic gradient i_{crit}, all stresses in the sand column are lost and the sand is free of any stresses.

Hence, if no surcharge filter is used, the sand column should collapse above its total length l at once when the hydraulic gradient i reach the critical value i_{crit}.

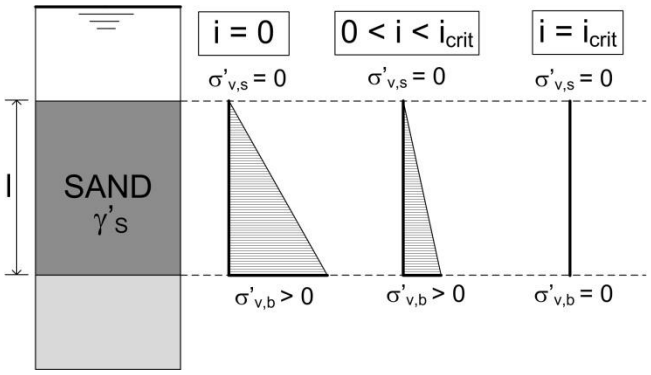

Figure 2: Stress level in the sand column without surcharge filter

Vertical effective stresses with surcharge filter

Figure 3 shows the vertical stresses in the sand column and in the surcharge filter for different hydraulic gradients i if a surcharge filter with defined thickness d_F is placed on the top of the sand column. For the determination of the stress levels illustrated in Figure 3, the buoyant unit weight of the surcharge filter γ'_F is approximately equal to the buoyant unit weight of the sand γ'_S.

Prior to the test (no flow forces acting on the sand), the effective vertical stresses rise with depth. The vertical effective stresses on the base of the sand column is $\sigma'_{v,b} = \gamma'_F \cdot d_F + \gamma'_S \, l$. On the top of the sand column, directly below the surcharge filter, the vertical effective stresses can be calculated by $\sigma'_{v,s} = \gamma'_F \cdot d_F$. Due to the coarseness of the used filter material, the surcharge filter has no influence on the fluid flow and therefore the effective vertical stresses on the top of the sand column, directly below the surcharge filter, always has the same value, independent of the hydraulic gradient i.

If the hydraulic gradient i has a certain value between zero and the critical hydraulic gradient i_{crit}, the effective vertical stresses on the base of the sand column are defined by $\sigma'_{v,b} = \gamma'_F \cdot d_F + \gamma'_S \cdot l - \Delta h \, \gamma_w$. Hence, the effective vertical stresses on the base of the sand column get reduced by potential difference Δh.

If the hydraulic difference Δh reaches the critical value Δh_{crit} (critical hydraulic gradient i_{crit}), the vertical effective stresses on the base of the sand column drops to zero ($\sigma'_{v,b}$ = 0), but in the residue sand column effective stresses are still acting.

Therefore, if a surcharge filter is installed, the sand column should collapse at the base of the sand column and should be up-lifted in total.

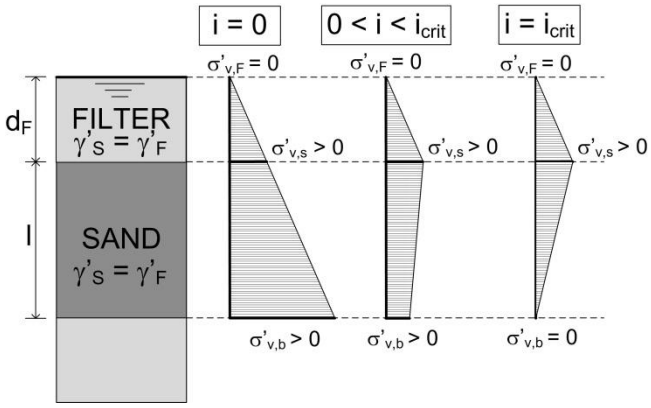

Figure 3: Stress level in the sand column with surcharge filter

Results of Experimental Series

For a better understanding of the fracture behavior of the sand, the test results were analyzed in detail. Therefore, the measured data are used to describe the fracture behavior of the sand column depending on the thickness of the surcharge filter d_F and the relative density D. Furthermore, by the use of visual monitoring (video and photo camera) it was possible to observe the course of fracture accurately.

Observed fracture behavior

Depending on the relative density D of the sand and the thickness of the surcharge filter d_F, different fracture modes were found. These fracture modes are described in the Tables 1, 2 and 3. Furthermore, for better understanding, Figure 4 and 5 illustrate the different fracture modes.

If no surcharge filter was used, the sand columns collapsed along their total height by local piping (Figure 5). If the sand had a low relative density D, the collapse was initiated by small cracks before the critical hydraulic gradient i_{crit} was reached. In the test with a high relative density D and without surcharge filter, the test collapsed suddenly after first small cracks were developed without a further rise of the potential difference Δh.

Table 1: Course of fracture (relative density D = 0.1)

surcharge filter thickness d_F [cm]	course of fracture
0	At first, small flow channels were observed in the whole sand column. With an increase of the potential difference, the flow channels exceed until the sand column collapsed by local piping.
1 and 2	The experiment collapsed suddenly by local piping. Also the surcharge filter was breached locally.
3	At the bottom of the sand column, the sand began to reduce into a fluid state. The fluidized area spread from the bottom up to a certain height, where the surcharge filter had a significant influence. At this elevation, the sand column cracks and the upper part was lifted up undisturbed with the surcharge filter. After a certain time, the surcharge filter was breached by local piping.
4, 5 and 6	At the bottom of the sand column, the sand began to reduce into a fluid state. The fluidized area spread from the bottom up to a certain height, where the surcharge filter had a significant influence. At this elevation, the sand column cracks and the upper part was lifted up with the surcharge filter.

If a surcharge filter was placed on the top, the tests collapsed at the base of the sand column (Figure 4). Upon the uplift of the sand column, the lower part of the sand column was fluidized and a crack between the intact part of the sand and the fluidized sand was developed. The height of the fluidized sand and the extend of the crack was depending on the thickness of the surcharge filter d_F and the relative density D. At the tests with a low relative density D and/or a small thickness of the surcharge filter d_F, the magnitude of the fluidized area was large. With a relative density of D = 0,8 and with a thickness of the surcharge filter of d_F = 3 to 6 cm, the sand column was uplifted without any liquefaction of the sand (no fluidized sand).
Hence, the observed course of fraction in the test series corresponds to the theoretical approach.

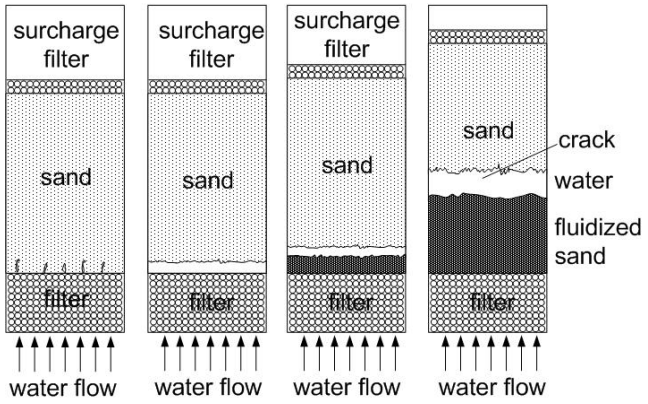

Figure 4: Course of fracture at the tests with D = 0.1, 0.5 and 0.8 as well as d_F = 1 to 6 cm

Table 2: Course of fracture (relative density D = 0.5)

surcharge filter thickness d_F [cm]	course of fracture
0	The experiment collapsed suddenly by local piping.
1, 2, 3, 4 and 5	Primarily small pipes occurred at the bottom of the sand column. Later on, the pipes raised and a crack between the fluidized and the uplifted sand was created. The crack grew and also increased to the top while the upper layer was lifted up.
6	A crack occurred suddenly between the filter layer on the bottom and the sand column. The crack grew and also increased to the top while the upper layer was lifted up.

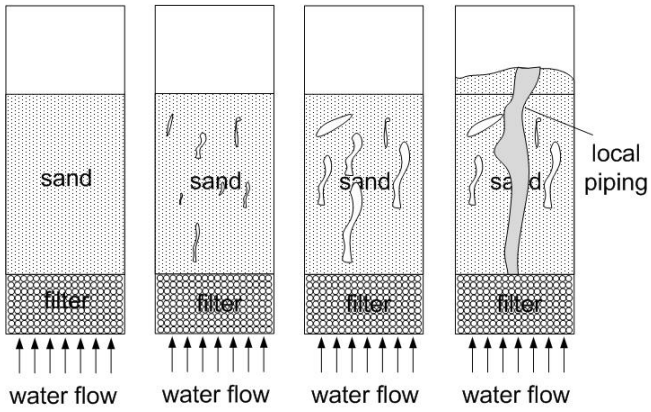

Figure 5: Course of fracture at the tests with D = 0.1, 0.5 and 0.8 as well as d_F = 0 cm

Table 3: Course of fracture (relative density D = 0.8)

surcharge filter thickness d_F [cm]	course of fracture
0	The experiment collapsed by local piping.
1, 2, 3 and 4	Primarily small pipes occurred at the bottom of the sand column. Later on, the pipes raised and a crack was developed between the fluidized and the uplifted sand. The crack was growing and was also increasing to the top while the upper layer was lifted up.
5 and, 6	A crack occurs suddenly between the filter layer on the bottom and the sand column. The crack was growing and was also increasing to the top during the upper layer was lifted up.

Critical hydraulic gradient

Additionally to the observation of the course of fracture, the critical hydraulic gradient i_{crit} was determined in each test. Therefore, the test series was applied to identify the critical hydraulic gradient i_{crit} depending on the relative density D and the thickness of the surcharge filter d_F.

Figure 6 displays the results of the uniaxial flow tests with different relative densities D = 0.1, 0.5 and 0.8. Moreover, the figure shows the theoretical critical hydraulic gradient $i_{crit,theoretical}$. Hence, the figures display the difference between the test results and the theoretical approach.

The results of the test series show that the critical hydraulic gradient i_{crit} depends heavily on the thickness of the surcharge filter d_F. With increasing thickness of the surcharge filter d_F, the critical hydraulic gradient i_{crit} increase disproportionately. The increase of the possible hydraulic gradient i_{crit} results from the additional stresses in the sand because of the load from the surcharge filter. Why the increase of the critical hydraulic gradient i_{crit} is disproportionate has to be analyzed in further investigations.

Also the relative density D of the sand has a significant influence on the critical hydraulic gradient i_{crit}. If the sand has a low relative density (D = 0.1), the critical hydraulic gradient i_{crit} is smaller than theoretically calculated (Figure 6). In the test series with a relative density of D = 0.5 and 0.8, the critical hydraulic difference Δh_{crit} and therefore the critical hydraulic i_{crit} is always higher than the theoretically predicted (Figure 6).

One reason for this phenomenon is that the buoyant unit weight of the sand and of the surcharge filter is growing with increasing relative density D. Therefore, the buoyant weight of the sand column increases with the relative density D. Hence, the possible critical hydraulic gradient i_{crit} increases with the relative density D.

Moreover, the friction angel φ increase with the relative density D and therefore the friction forces in the sand and between the sand and the cylinder wall are increasing. This also allows higher possible hydraulic gradients i_{crit}.

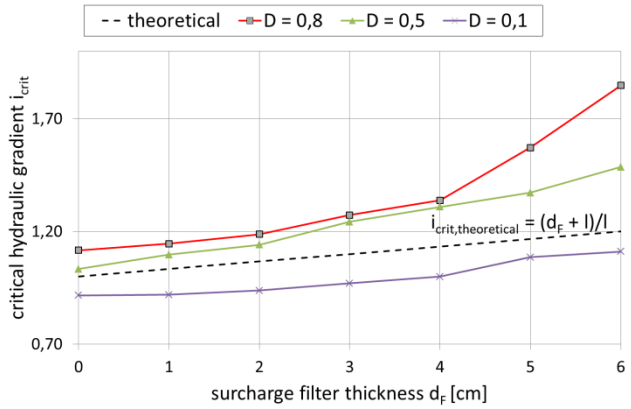

Figure 6: Critical hydraulic gradient i_{crit}

Measured data

The sand column was observed during each test through several measurement techniques. Hence, the water pressure was observed at three different levels (Figure 1) at the edge of the sand column by water pressure sensors. Figure 7 displays the water pressure in the middle of the test box for the test with d_F = 4 cm and D = 0.8. Both water pressure sensors show approximately the same values. The small difference is caused from the uncertainty of the sensors. The water pressure rises stepwise according to the potential difference Δh. Through the abrupt rise in pressure, the collapse of the sand column becomes apparent (marked in Figure 7). The same water pressure curves were observed by almost all tests with surcharge filter.

The only exceptions are the tests with a low relative density D and without or with small thickness of the surcharge filter. In these tests, the collapse was not abrupt, but gradual. Therefore the water pressure sensors display irregulars in the total time interval of the collapse.

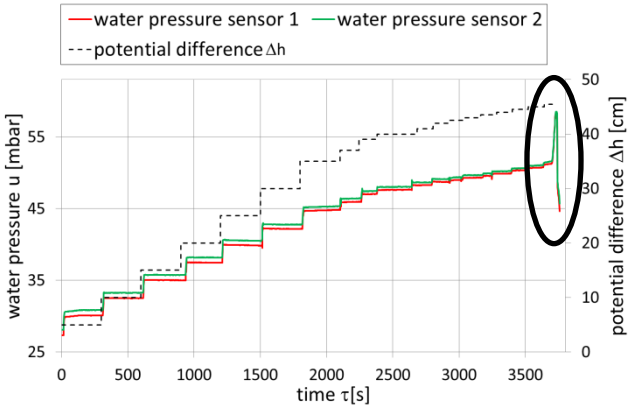

Figure 7: Water pressure conditions in the middle of the test cylinder during the test with d_F = 4 cm and D = 0

Moreover, the elevation of the surcharge filter was measured by two displacement transducer during each test. The transducer was placed on the top of the surcharge filter. The elevation was only measured at tests with surcharge filters. This was the case, because in the tests without a surcharge filter, the transducer was settled into the sand.

In all tests with an installed surcharge filter the displacement transducers show little displacements at the start of each test. Figure 8 shows for example the elevation of the test with d_F = 4 cm and D = 0.8. Later on, the curve runs horizontally. The collapse becomes apparent if the transducers show relevant elevation. The same course of fracture was observed in all tests with surcharge filter.

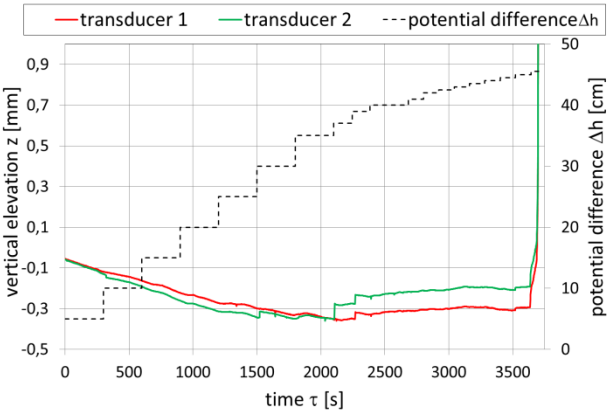

Figure 8: Elevation of the surcharge filter during the test with d_F = 4 cm and D = 0.8

The water pressure sensors as well as the displacement transducer show an abrupt collapse of the sand column for nearly all tests with surcharge filters. Only if the sand column has a low relative density D and a small thickness of the surcharge filter d_F, the collapse happens over an certain period of time.

Conclusion

Numerous laboratory 1D-flow tests were executed to analyze the influence of the thickness of the surcharge filter d_F and the relative density D on the fracture behavior at uniaxial flow tests. Therefore, the relative density D of the sand and the thickness of the surcharge filter d_F was varied.

The observations of the fracture behavior confirm the theoretical approach. Hence, the sand column collapsed without surcharge filters over the total height of the sand column by local piping. If a surcharge filter was used, the sand column cracked at the base and was lifted up in total.

Moreover, the critical hydraulic gradient i_{crit} depends heavily on the thickness of the surcharge filter d_F. With increasing thickness of the surcharge filter d_F, the critical hydraulic gradient i_{crit} increases disproportionately.

This results from the additional stresses and therefore the additional friction forces in the sand and between the sand and the wall of the test cylinder because of the surcharge filter.

Figure 3 shows, that in the critical state the stresses at the base of the sand column drop to zero. Nevertheless, in the other parts of the sand column stresses are still acting. These stresses result in friction forces between the sand and the wall of the test cylinder. With a thicker surcharge filter, the stresses in the sand acting deeper in the sand column and the friction forces between the sand and the wall of the test cylinder get higher. Hence, the necessary critical hydraulic difference Δh_{crit} to initiate the collapse of the sand column gets higher.

Why the possible critical hydraulic gradient i_{crit} increase disproportionate with the thickness of the surcharge d_F filter has to be analyzed in further investigations.

Additionally, the relative density D of the sand column has an influence on the critical hydraulic gradient i_{crit}. One reason for the phenomena is that the friction angle of the sand depends heavily on the relative density D. With increasing relative density D also the possible friction forces between the sand particles and between the sand column and the wall of the test cylinders increase. Moreover, the buoyant unit weight of the sand and the surcharge filter increase with rising relative density D.

To analyze the stresses in the sand column in more detail, the Universität der Bundeswehr München will execute uniaxial flow tests with glass balls as a first step. These tests will be simulated with the Discrete Element Method Software (DEM).

References

Odenwald, B., Herten, M., 2008. Hydraulischer Grundbruch: neue Erkenntnisse, Bautechnik 85, Heft 9, S. 585 -595.

Schober, P., 2011. Hydraulic heave at excavation walls with under-flow of small embedded depth and filer layers at the excavation side of the wall, 21th EYGEC 2011, Rotterdam, The Netherlands.

Schober, P., Boley, C., Odenwald, B., 2011. Hydraulic Heave safety at Excavation Walls with Surcharge filters, ISGSR 2011, Munich

Terzaghi, K, Peck, R. B., 1948. Soil Mechanics in Engineering Practice, John Wiley and Sons, New York

Tanaka, T., Toyokuni, E., 1991. Seepage-Failure Experiments on Multi-Layered Sand Columns: Effects of Flow Conditions and Residual Effective Stresses on Seepage-Failure Phenomena, Soil and Foundation, The Japanese Geotechnical Society, Vol. 31(4), Page 13-36